DOI 10.1007/s11041-017-0180-3
Metal Science and Heat Treatment, Vol. 59, Nos. 7 – 8, November, 2017 (Russian Original Nos. 7 – 8, July – August, 2017)

UDC 549.6:669.715

EFFECT OF ZIRCON PARTICLE SIZE ON AGE HARDENING BEHAVIOR OF A356 ALLOY BASED COMPOSITES

T. Satish Kumar,[1, 4] R. Subramanian,[1] S. Shalini,[2] A. Gowrishankar,[1] and P. C. Angelo[3]

Translated from *Metallovedenie i Termicheskaya Obrabotka Metallov*, No. 8, pp. 37 – 40, August, 2017.

Melt stirring was used to introduce various amounts of zircon ($ZrSiO_4$) particles of various sizes into aluminum alloy A356 of the Al – Si system. The effect of zircon particle sizes on age hardening behavior of stir-cast A356 alloy/zircon reinforced composites was studied by measuring microhardness after solution treatment and aging for various times. The structure of composites was studied by methods of optical microscopy, x-ray diffraction, scanning electron microscopy combined with energy dispersive x-ray spectroscopy, and high-resolution transmission electron microscopy. The addition of zircon was found to accelerate age hardening of the matrix alloy. It is established that the maximum hardness increases and the time of attaining this maximum decreases with growing content of zircon particles and with reduction in their average size.

Key words: aluminum alloys, zircon particles, composite, stir casting, age hardening.

INTRODUCTION

Aluminum A356 alloy based composites are widely used in automotive and aerospace industry due to light weight, high specific strength, high modulus, and excellent wear resistance [1]. Many of these composites are based upon the age-hardenable aluminum alloy matrix reinforced with ceramic particles such as SiC and Al_2O_3 [2 – 4]. It is well known that these reinforcements can accelerate the aging kinetics of the matrix alloy due to higher matrix dislocation densities in the composites. Since matrix dislocations act as nucleation sites for precipitates, higher dislocation densities facilitate enhanced precipitation. In addition, dislocations act as preferential paths for solute diffusion, thus further accelerating the aging kinetics [3]. The aging behavior of aluminum matrix composites reinforced with various particles has being studied, including the age hardening behavior of various ceramic-reinforced A356 alloy based composites. Study of the hardening behavior of A356 alloy reinforced with Al_2O_3 particles [5] showed that the precipitation kinetics was enhanced by addition of these particles. Earlier, similar behavior was observed in A356 alloy reinforced with glass particles [6]. The mechanical properties of A356 aluminum alloy can be significantly improved by appropriate heat treatment, in particular, using the T6 regime in which alloy strengthening is achieved through the precipitation of Mg_2Si phase in the aluminum matrix during artificial aging [7, 8]. Precipitation hardening also occurs in the aluminum matrix saturated with silicon and magnesium in the solid solution [9, 10]. Ceramic reinforcement of Al – Cu – Mg alloy caused acceleration of the aging kinetics as compared to the unreinforced matrix alloy, thus reducing energy consumption [11 – 13].

There is increasing interest in aluminum-based composites with reinforcement agents that are lower in cost and can provide better properties, an example being the possible use of zircon ($ZrSiO_4$) possessing high hardness and modulus of elasticity, good thermal stability and wear resistance, and a very low thermal expansion coefficient compared to that of most other ceramic oxides [14]. To the best of the authors' knowledge, there are no reports on the effect of zircon particles on aging behavior of A356 alloy. In this context, the present work was aimed at studying the effect of zircon particles amount and size on aging behavior of A356 alloy. As zircon possesses a very low thermal expansion coefficient compared to other ceramics, the thermal mismatch between the aluminum alloy matrix and reinforcement particles will increase during quenching and that may lead to better aging characteristics of composites for the aforementioned reasons.

[1] Department of Metallurgical Engineering, PSG College of Technology, Coimbatore, India.
[2] Department of Physics, PSG College of Technology, Coimbatore, India.
[3] Metal Testing & Research Centre, PSG College of Technology, Coimbatore, India.
[4] E-mail: thandalamsatish@gmail.com.

TABLE 1. Designation and Composition of Specimens Prepared by Stir Casting

Composite	Content of coarse particles (74 – 100 μm), wt.%	Composite	Content of fine particles (37 – 44 μm), wt.%
A1	5	B1	5
A2	10	B2	10
A3	15	B3	15

Thus, the effect of zircon on the aging behavior of the matrix alloy has been studied and reported here for the first time.

METHODS OF STUDY

In the present investigation, A356 alloy is used as the matrix the composition of which includes 7.5% Si, 0.4% Mg, 0.3% Fe, 0.2% Cu, 0.1% Zn, 0.1% Ni, and 90.9% Al. The composites were synthesized by introducing fine (37 – 44 μm) and coarse (74 – 100 μm) zircon particles at variable content of 5, 10 and 15 wt.% into A356 alloy matrix through melt stirring in furnace at a temperature of 750°C. The base alloy contains 0.6 wt.% Mg, which is responsible for wettability between the matrix and reinforcement. In order to enhance the wettability, about 0.6 wt.% Mg was added to the melt [15]. Zircon particles were preheated at a temperature of 450°C for 2 h to eliminate the residual moisture. Required amounts of preheated zircon particles were then added to the melt at a rate of about 10 g/min with continuous stirring for 10 min by stirrer rotating at 700 rpm. Then, the melt was poured into identical steel molds. Designation of the composites synthesized with different size and content of zircon particles is given in Table 1.

From available literature, it is known that 15 wt.% of reinforcing addition into the matrix results in better properties of the composites [14, 16 – 18]. For this reason, the content of reinforcement agent (zircon) in composites in the present study was also restricted to 15 wt.%.

Aging studies were carried out in order to optimize the time to achieve peak hardness of the unreinforced alloy and related composite specimens annealed at a selected temperature of 180°C. Stir-cast specimens were initially solutionized for 4 h at 540°C, then quenched in cold water, and finally aged at 180°C for various periods of time. The solutionizing temperature of 540°C was chosen based on the phase diagram of Al – Si alloys [19]. Vickers microhardness (*HV*) measurements were performed for the age hardened alloy and composites using a Zwick microhardness tester at a load of 1 kgf (10 N) and a dwell time of 15 sec. Five readings were taken for each specimen and the average hardness values were calculated.

Optical microscopy was used to study the distribution of zircon particles in A356 alloy matrix. Microstructural analysis was carried out for both the unreinforced alloy and as-cast composite specimens in order to investigate the solidification microstructure, distribution of zircon particles, and presence of porosity. Samples were polished well, etched with Keller's reagent, and examined in a Carl Zeiss optical microscope.

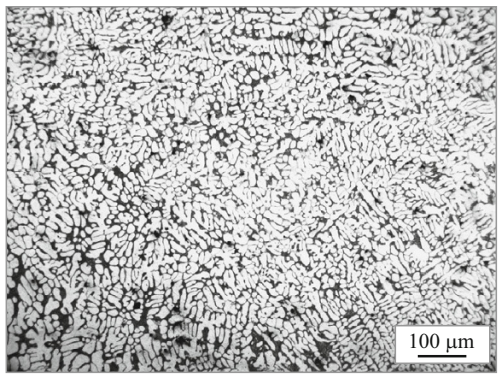

Fig. 1. Optical micrograph of as-cast A356 alloy.

X-ray diffraction (XRD) analysis was carried out on Shimadzu XRD 6000 x-ray diffractometer using CuK_α (λ = 1.5409 Å) radiation. Each sample was scanned over 2θ angles ranging from 10 to 80°. The angles of characteristic peaks of various phases were measured and indexed using JCPDF database.

Scanning electron microscopy (SEM) combined with energy dispersive x-ray (EDX) spectroscopy was used to study the formation of Mg_2Si precipitates. The age hardened alloy and composites were examined in JSM-5800 (JEOL) equipped with EDX attachment. SEM images were taken in the electron-backscattering mode.

High-resolution transmission electron microscopy (HRTEM) analysis was performed in JEM 2100 (JEOL) microscope operating at 200 kV. Analysis was performed for 3-mm samples taken from the transverse section of each as-cast specimen. Samples for analysis were prepared by mechanical polishing, followed by electrolytic thinning with perchloric acid – ethanol solution at room temperature.

RESULTS AND DISCUSSION

Figure 1 presents an optical micrograph of as-cast unreinforced monolithic A356 alloy, which shows the presence of silicon particles in the interdendritic regions of α-Al matrix.

Optical micrographs of the microstructure of composites A1 – A3 and B1 – B3 are shown in Fig. 2*a* – *c* and *d* – *f*, respectively. In comparison to the as-cast monolithic A356 alloy (Fig. 1), the microstructure of all composites shows evidence of the refinement of α-Al based solid solution dendrites. The refinement in dendritic arms can be attributed to their growth restricted by introduced particles [14, 16, 20]. Zircon particles are distributed more or less uniformly in the alloy matrix, which favors achieving high hardness of the composite. In addition, the refinement of dendritic structure also leads to an increase in hardness of the composite.

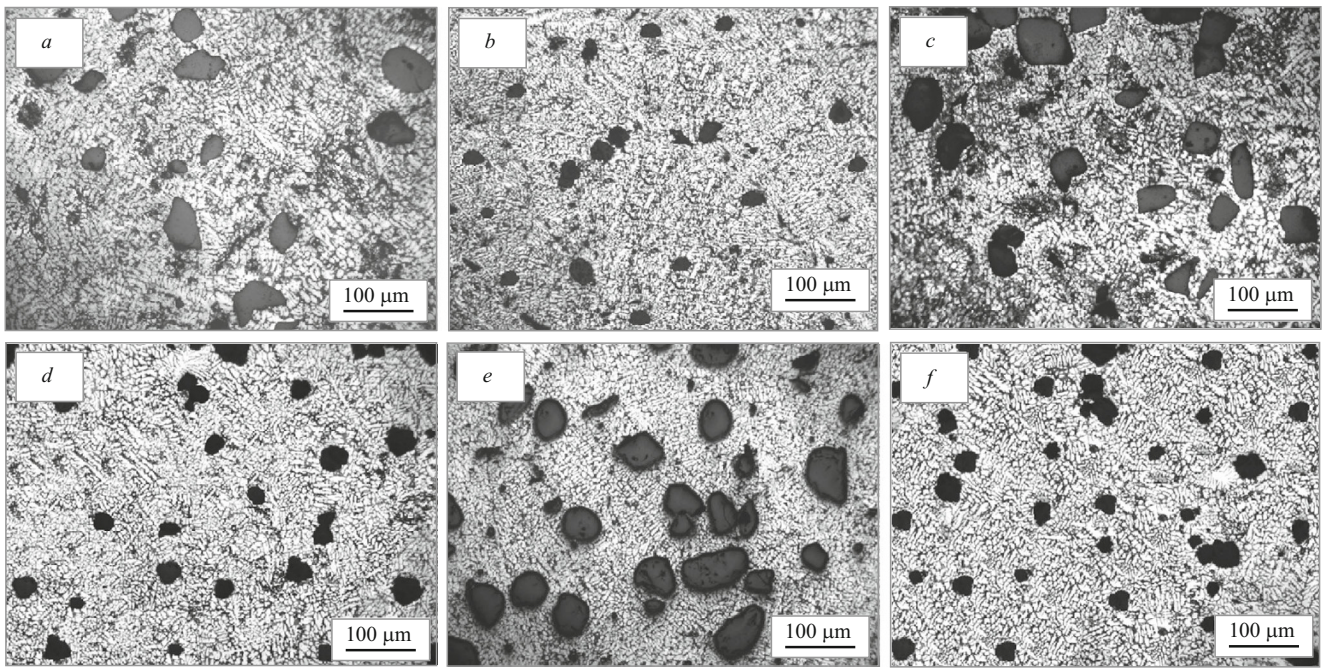

Fig. 2. Optical micrographs of composites A1 (*a*), A2 (*b*), A3 (*c*), B1 (*d*), B2 (*e*), and B3 (*f*).

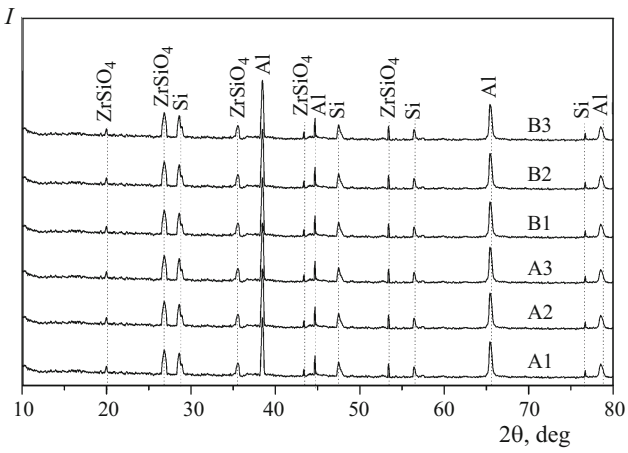

Fig. 3. XRD patterns of as-cast composites (*I* is the reflection intensity).

Figure 3 shows XRD patterns of all composites. These patterns reveal the presence of Al, Si, and $ZrSiO_4$. Note that, since the content Mg in composites is low, reflections of magnesium phases are not manifested.

Figure 4 presents a SEM image of the microstructure of A3 composite and the corresponding EDX spectrum of dark Mg_2Si precipitates on eutectic silicon particles. During artificial aging at 180°C, dark Mg_2Si phase precipitates with lamellar or "Chinese-script" shape morphology. Similar morphology was observed in other specimens studied in this work and reported [21] in the study on AlSi1MgMn aluminum-based alloy.

Commonly accepted order of decomposition of a supersaturated solid solution, leading to precipitation of the Mg_2Si phase, is as follows [2, 22]: supersaturated solid solution (SSS) → (Mg + Si) cluster → primary Guinier–Preston (GP) zones → lamellar/plate-like GP zones → β″-needles → β′-rods + Si + others → β-plates + Si.

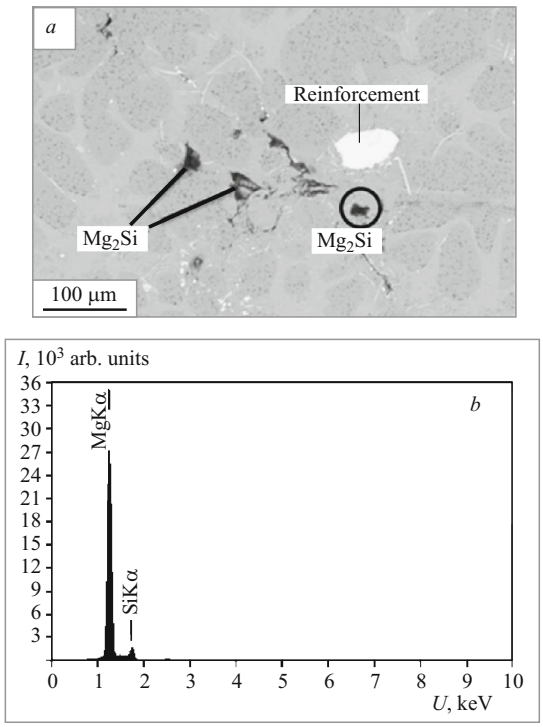

Fig. 4. SEM image of the microstructure of A3 composite ("reinforcement" is the hardening zircon particle) (*a*) and EDX spectrum of Mg_2Si particles (*b*).

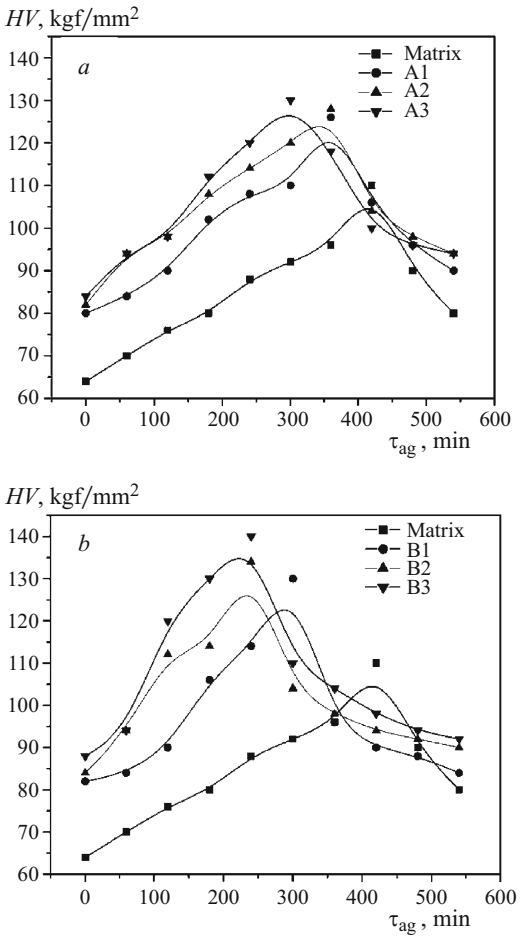

Fig. 5. Plots of the Vickers hardness *HV* of A356 alloy matrix and related composites vs. duration τ_{ag} of aging at 180°C: *a*) composites with 74 – 100 μm zircon particles; *b*) composites with 37 – 44 μm zircon particles.

Figure 5 illustrates the influence of the size and content of zircon particles on the aging behavior of A356 alloy and related composites. From these curves it can be seen that microhardness of the composites is higher than that of the monolithic alloy, and that the hardness grows with increasing content of zircon particles. The time to achieve the peak hardness in all composites is shorter compared to that in Zr-free alloy, and it decreases with increasing content of zircon particles. The accelerated aging kinetics of the composite can be due to increased dislocation density in the matrix during quenching after the solid solution heat treatment. Analogous acceleration of the attaining of maximum hardness in reinforced composites was observed in [23]. Composites with 37 – 44 μm zircon particles exhibit most pronounced age hardening, followed by composites with 74 – 100 μm particles and Zr-free alloy. Slower kinetics of aging and lower peak hardness in composites with increasing zircon particle size was also reported in [24].

CONCLUSIONS

Composites based on A356 aluminum alloy reinforced with zircon ($ZrSiO_4$) particles were obtained by stir casting technique. Microstructural examination revealed the uniform distribution of zircon particles in the alloy matrix. From the aging studies, it was found that addition of zircon particles accelerated age hardening and increased the peak hardness as compared to the monolithic alloy. It is established that the hardening process accelerates and the peak hardness grows with increasing content and decreasing size of introduced zircon particles.

REFERENCES

1. N. Sree Harsha, S. Sankaran, and B. S. Murty, *Trans. Indian Inst. Met.,* **64**, 123 (2011).
2. R. Appendino, C. Badini, F. Marino, and A. Tomasi, *Mater. Sci. Eng. A*, **135**, 275 (1991).
3. M. Gupta and M. K. Surappa, *Mater. Res. Bull*., **30**, 1023 (1995).
4. I. Dutta, S. M. Allen, and J. L. Hafley, *Metall. Trans. A,* **22A**, 2553 (1991).
5. A. Daoud and W. Reif, *J. Mater. Process. Technol*., **123**, 313 (2002).
6. Z. M. El-Bradie and A. N. Abd El-Azim, *J. Mater. Process. Technol*., **66**, 73 (1997).
7. M. Abdulwahab, I. A. Madugu, S. A. Yaro, et al., *Mater. Des.,* **32**, 1159 (2011).
8. S. Tahamtan, M. A. Golozar, F. Karimzadeh, and B. Niroumand, *Mater. Charact*., **59**, 223 (2008).
9. A. M. Kliauga, E. A. Vieira, and M. Ferrante, *Mater. Sci. Eng. A*., **480**, 5 (2008).
10. D. L. Zhang, *Mater. Sci. Forum*, **217**, 771 (1996).
11. V. K. Varma, Y. R. Mahajan, and V. V. Kutumbarao, *Scr. Mater.*, **37**, 485 (1997).
12. R. J. Arsenault, L. Wang, and C. R. Feng, *Acta Metall. Mater.*, **39**, 47 (1991).
13. S. W. Kim, U. J. Lee, S. W. Han, et al., *Composites Part B: Eng.*, **34**, 737 (2003).
14. E. G. Okafor and V. S. Aigbodion, *Tribol. Industry*, **32**, 31 (2010).
15. A. Banerji, M. K. Surappa, and P. K. Rohatgi, *Metall. Trans. B*, **14B**, 273 (1983).
16. S. Kumar, V. Sharma, R. S. Panwar, and O. P. Pandey, *Tribol. Lett.,* **47**, 231 – 251 (2012).
17. J. Hashim, *Jurnal Teknologi*, **35A**, 9 – 20 (2001).
18. S. K. Chaudhury, A. K. Singh, C. S. Sivaramakrishnan, and S. C. Panigrahi, *Wear*, **258**, 759 – 767 (2005).
19. J.L. Murray and A. J. McAlister, *Bull. Alloy Phase Diagr.*, **5**, 74 – 77 (1984).
20. D. Siva Prasad, C. Shoba, and N. Ramanaiah, *J. Mater. Res. Technol.*, **3** (1), 79 – 85 (2014).
21. I. Bobic, J. Ružic, B. Bobic, et al., *Mater. Sci. Eng. A*, **612**, 7 – 15 (2014).
22. G. M. Nowotnik, J. Sieniawski, and M. Wierzbinska, *J. Achiev. Mater. Manuf. Eng.*, **20**(1 – 2), 155 – 158 (2007).
23. S. H. Nandam, B. S. Murty, and S. Sankaran, *Metall. Mater. Trans. A*, DOI: 10.1007/s11661-015-2927-z (2015).
24. B. Dutta and M. K. Surappa, *Scr. Metall. Mater.*, **32**(5), 731 – 736 (1995).